Microbial Ecology

Stability in a Denitrifying Fluidized Bed Reactor

M. Gentile[1], T. Yan[2], S.M. Tiquia[2,3], M.W. Fields[4], J. Nyman[1], J. Zhou[2] and C.S. Criddle[1,5]

(1) Department of Civil and Environmental Engineering, Stanford University, Stanford, CA, USA
(2) Environmental Science Division, Oak Ridge National Lab, Oak Ridge, TN, USA
(3) Department of Natural Sciences, The University of Michigan, Dearborn, MI, USA
(4) Department of Microbiology, Miami University, Oxford, OH, USA
(5) Department of Civil and Environmental Engineering, M11 Terman Engineering, 380 Panama Mall, Stanford, CA 94305-4020, USA

Received: 22 December 2004 / Accepted: 9 March 2005 / Online publication: 28 July 2006

Abstract

This study evaluates changes in the microbial community structure and function of a pilot-scale denitrifying fluidized bed reactor during periods of constant operating conditions and periods of perturbation. The perturbations consisted of a shutdown period without feed, two disturbances in which biofilms were mechanically sheared from carrier particles, and a twofold step increase in feed nitrate concentration. In the absence of perturbations, nitrate removal was stable and consistently greater than 99%. The structure and dynamics of the microbial community were studied using cloning and sequencing techniques and terminal restriction fragment length polymorphism (T-RFLP) of the SSU rRNA gene. Under unperturbed operating conditions, stable function was accompanied by high constancy and low variability of community structure with the majority of terminal restriction fragments (T-RFs) appearing throughout operation at consistent relative abundances. Several of the consistently present T-RFs correlated with clone sequences closely related to *Acidovorax* (98% similarity), *Dechloromonas* (99% similarity), and *Zoogloea* (98% similarity), genera recently identified by molecular analyses of similar systems. Significant changes in community structure and function were not observed after the shutdown period. In contrast, following the increase in loading rate and the mechanical disturbances, new T-RFs appeared. After both mechanical disturbances, function and community structure recovered. However, function was much more resilient than community structure. The similarity of response to the mechanical disturbances despite differences in community structure and operating conditions suggests that flexible community structure and potentially the activity of minor members under non-perturbation conditions promotes system recovery.

Correspondence to: C.S. Criddle; E-mail: ccriddle@stanford.edu

Introduction

The maintenance of stable function is the goal of system design and operation for bioremediation and biological wastewater treatment. A fundamental understanding of the relationship between functional stability and microbial community dynamics could be an essential component of designing and operating stable treatment systems [2, 6]. Such an understanding could allow for improvement of engineering models for treatment system design, determination of candidate populations for bioaugmentation or genetic manipulation, and establishment of rigorous methods for monitoring and controlling bioreactor systems.

The relationship between community dynamics and functional stability under unperturbed operating conditions has been explored in a variety of reactor systems. The microbial communities in some systems were unstable with intermittently present populations and many fluctuations in dominance [12, 39, 48], whereas the microbial communities in other systems were stable with many continuously present populations and fewer fluctuations in dominance [35, 44]. The reason for this apparent disparity among systems remains unclear.

In practice, bioreactors rarely experience steady conditions and are often subject to changes in operational parameters and disturbances, but little is known about how such disturbances affect community dynamics and, in turn, functional stability. Results from the few studies that have examined the microbial community in response to disturbances have demonstrated a shift in community structure [13, 17, 37, 40]. In some cases, community structure was resilient [13, 17, 37], meaning

that it eventually returned to its original state following disruption [16, 32].

Denitrification is a critical process in many engineering applications including nitrogen removal from wastewater and bioremediation of polluted groundwater [18, 21, 36]. However, investigation of community dynamics in denitrifying systems has been somewhat limited. Community analysis results from a methanol-fed denitrifying FBR over a short time scale (11 weeks) revealed that a stable community was established after start-up [24]. Less is known about community dynamics in denitrifying systems over longer time scales.

In this investigation, a pilot-scale denitrifying fluidized bed reactor (FBR) fed lactate and ethanol was examined. This pilot-scale reactor was used as an inoculum for a field-scale FBR at the Field Research Center (FRC) in Oak Ridge, Tennessee [19]. The FBR at the FRC is currently one of many treatment steps used in remediation experiments on groundwater contaminated with nitrate and uranium. During a 370-day period of operation, the pilot-scale FBR was subjected to several periods of constant operating conditions as well as operational changes and disturbances. Microbial community structure and function were stable under constant operating conditions. In response to disturbance, both function and community structure were resilient, although on different time scales.

Methods

FBR Parameters. The pilot-scale FBR consisted of a glass column with a recycle line for fluidization as detailed in Table 1. Granular activated carbon was used as the biofilm carrier. The FBR was inoculated with a denitrifying enrichment culture developed from groundwater from well TPB-16 at the FRC [19]. The groundwater in well TPB-16 had a circum neutral pH and moderate nitrate levels (30 mg/L).

FBR Feed Solutions. The reactor received two separate, nonsterile feed streams, one for nitrate plus nutrients and the other for lactate and ethanol. Initially, the nitrate feed contained 3.02 g/L of $NaNO_3$, 30 mg/L of $Na_3P_3O_9$, 20 mg/L of $NaSO_4$, 30 mg/L $MgCl_2{\cdot}6H_2O$, 0.3 mg/L of $FeCl_2{\cdot}4H_2O$, 0.1 mg/L of $ZnSO_4{\cdot}7H_2O$, 85 μg/L of $MnSO_4{\cdot}H_2O$, 60 μg/L of H_3BO_3, 19 μg/L of $CoCl_2{\cdot}6H_2O$, 4 μg/L of $CuSO_4{\cdot}5H_2O$, 28 μg/L of $NiSO_4{\cdot}6H_2O$, and 40 μg/L of $Na_2MoO_4{\cdot}2H_2O$. As the sodium nitrate concentration was increased later in operation, the concentrations of $Na_3P_3O_9$, $NaSO_4$, and $MgCl_2{\cdot}6H_2O$ were increased proportionally, whereas all other nutrients were held at their original concentrations. The concentration of the lactate and ethanol were adjusted to minimize the chemical oxygen demand (COD) in the effluent and ensure complete reduction of nitrate and nitrite. This was accomplished using a COD/N ratio for the combined feeds of 4.0 to 6.3 g COD/g N. The electron donor feed consisted of equal concentrations of lactic acid and ethanol on a COD basis.

Table 1. FBR physical dimensions and operational parameters

Diameter (cm)	6.4
Bed volume (L)[a]	6.4
Total volume (L)[b]	15.3
Bed porosity (%)	33–49
Linear velocity (cm/s)	1.3

[a]For fully expanded bed.
[b]Including recycle lines.

FBR Operational Parameters and Disturbances. Samples for microbial community analysis were collected over a period of 370 days, including several operational changes and disturbances (Fig. 1). Day zero of the period reported on in this study was 200 days after the FBR was inoculated. From day 33 to day 58, the FBR experienced a shutdown in which both feed pumps and the fluidization pump were off. For the first 180 days, the loading rate was 1.1–1.4 g N/L bed volume per day. From day 180 to day 192, the loading rate was increased through step increases in feed nitrate concentration. From day 192 to the end of the study, the loading rate was 2.7–2.9 g N/L bed volume per day. Disturbances on days 125 and 273 involved mechanical shearing of biofilms from carrier particles.

Analytical Methods. Nitrate and nitrite concentrations were measured using an ion chromatograph (Dionex, Sunnyvale, CA, USA). Nitrogen was quantified by a gas chromatograph with a thermal conductivity detector (Gow-Mac Instrument Company, Lehigh, PA, USA).

Microbial Community Analysis

DNA Extraction and Purification. Carrier particles with biofilms were removed from the reactor, centrifuged for 2 min at 16,000 × *g*, decanted, and stored at −20°C until analysis. For terminal restriction fragment length polymorphism (T-RFLP) analysis, DNA was extracted using an Ultraclean Soil DNA Isolation Kit according to the manufacturer's instructions (Mo Bio Laboratories, Solana Beach, CA, USA). A clone library was constructed from one portion of the biofilm sample archived on day 25. For clone library construction, the biomass was resuspended in a lysis buffer and the cells were disrupted using a previously described grinding method [47]. DNA was then extracted for clone library construction as previously described [20, 47], and was purified by gel electrophoresis plus a minicolumn preparation (Wizard DNA Clean-Up system, Promega, Madison, WI, USA) [47].

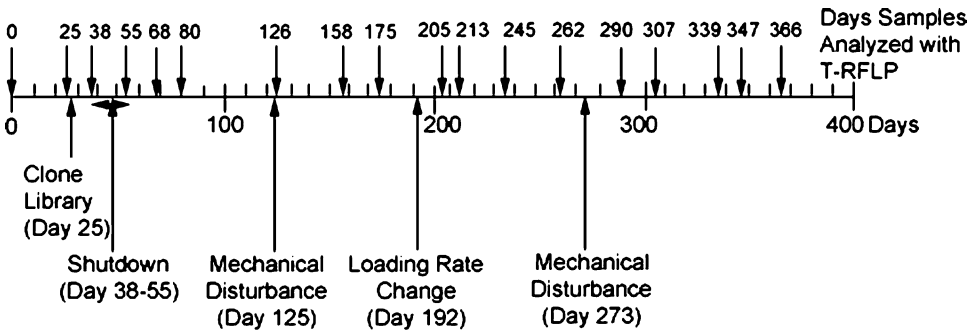

Figure 1. Timeline of FBR operational changes, disturbances, and community structure sampling events for the 370 days of this investigation. The mechanical disturbances on days 125 and 273 resulted in the shearing of biofilms from carrier particles.

Polymerase Chain Reaction Amplification and Purification. For clone library construction, the SSU rRNA genes were amplified in a 9700 Thermal Cycler (PerkinElmer, Wellesley, MA, USA) with the primer pair 8F (5′-AGAGTTTGATCCTGGCTCAG-3′) and 1540R (5′-AAGGAGGTGATCCAGCC-3′). The polymerase chain reactions (PCRs) (20 μL) contained 1× PCR buffer (50 mM KCl, 10 mM Tris–HCl, pH 9.0, and 0.1% Triton X-100), 1.8 mM $MgCl_2$, 80 ng bovine serum albumin (Boehringer Mannheim, Indianapolis, IN, USA), 0.25 mM 4× dNTPs (USB Corporation, Cleveland, OH, USA), 10 pmol each primer, 2.5 U *Taq* polymerase, and 1 μL purified DNA (5–10 ng). To minimize PCR-induced artifacts, the optimal number of cycles was determined and five PCRs were combined prior to cloning as described previously [33]. The PCR thermal cycling parameters were as follows: 80°C for 30 s, 94°C for 2 min; 94°C for 30 s, 58°C for 1 min, 72°C for 1 min, 26 cycles; 72°C for 7 min. PCR products were analyzed on 1.5% (w/v) Tris acetate–EDTA agarose gels, and the product size was confirmed. The combined PCR products were separated by electrophoresis in a low-melting-point agarose gel (0.8%). The appropriate band was excised and the DNA was recovered using a Wizard Prep Kit (Promega).

For T-RFLP, SSU rRNA genes were amplified in a PTC-150 MiniCycler™ (MJ Research, Waltham, MA, USA) from community DNA using primer pair 8F fluorescently labeled with hexachlorofluorescein (HEX) and 1392R (5′-ACGGGCGGTGTGTRC-3′) [25] (Qiagen Operon, Alameda, CA, USA). The PCRs (50 μL) contained 1× PCR buffer (100 mM KCl, 20 mM Tris–HCl, pH 8.0, 0.1 mM EDTA, 1 mM dithiothreitol, 50% glycerol, 0.5% Tween® 20, and 0.5% Nonidet® P40), 2.5 mM $MgCl_2$, 5% dimethyl sulfoxide, 0.4 mM 4× dNTPs (Invitrogen, Carlsbad, CA), 12.5 pmol each primer, and 40 ng of template DNA. Samples were denatured at 94°C for 5 min. Promega *Taq* DNA polymerase (1.5 U) in storage buffer B (Promega) was then added. The PCR thermal cycling parameters were as follows: 94°C for 45 s, 55°C for 30 s, 72°C for 1.5 min, 30 cycles; 72°C for 7 min. PCR products were analyzed on 1.8% (w/v) Tris borate–EDTA agarose gels, and the product size was confirmed. Products for three replicate PCR reactions were combined for each sample and purified with the Montage PCR Centrifugal Device (Millipore, Billerica, MA, USA).

Cloning, Sequence Determination, and Phylogenetic Analysis. The PCR products purified for clone library construction were resuspended in 6 μL ddH_2O. Two-microliter aliquots of PCR products were directly ligated to the pCR 2.1 vector obtained from Invitrogen (San Diego, CA, USA) and transformed [33] in *Escherichia coli* cells. All white colonies were picked and screened for desired gene inserts, which were detected with primers specific for the polylinker of the vector pCR 2.1.

PCR products (100 μL) were amplified from clones with vector-specific primers via colony PCR and were then purified with the ArrayIt™ PCR Purification Kit (TeleChem International, Inc., Sunnyvale, CA, USA) or treated with ExoSAP-IT™ (USB Corporation) according to the manufacturer's instructions. Partial sequences were obtained from the purified inserts with the SSU rRNA gene primer 529r (5′-CGCGGCTGCTGGCAC-3′) using an ABI PRISM BigDye Terminator kit (Applied Biosystems, Foster City, CA, USA) and an ABI PRISM 3700 DNA analyzer (PerkinElmer). DNA sequences were edited using the Sequencher™ program (v. 4.0, Gene Codes Corporation, Ann Arbor, MI, USA).

Clone sequences were aligned with SSU rRNA sequences from the Ribosomal Database Project (RDP) [3] in ARB [29]. A phylogenetic tree of clone sequences, closely related database sequences, and isolate sequences (discussed below) was constructed using the neighbor-joining method within PAUP version 4.0 with the sequence alignment exported from ARB. Bootstrap analysis and sequence similarity calculations were performed in PAUP. The abundance-based coverage estimator (ACE) in EstimateS was used to estimate species richness using a species definition of 97% sequence similarity [4].

Restriction Digests and T-RFLP Data Analysis. PCR product purified for T-RFLP analysis (95 ng/μL) was

cleaved with 0.25 U/μL of either *Rsa*I (Invitrogen) or *Msp*I (Promega) in buffer provided by the manufacturer for 2.5 h in a 37°C waterbath. Restriction digest products were analyzed on an ABI PRISM® 3100 Genetic Analyzer at the Genomics Technology Support Facility, Michigan State University.

T-RFLP profiles were standardized based on the methods of Dunbar and Kaplan [8, 23]. Total signal was calculated as the sum of peak heights. Profiles were standardized to the sample with the lowest total signal and peaks with adjusted heights lower than the threshold (50 units) were removed. The relative abundance of each T-RF was calculated as the ratio of peak height for that T-RF to the sum of peak heights for all T-RFs in the profile and expressed as a percentage. Histograms were prepared from relative abundance data. Principal component analysis (PCA) of T-RFLP profiles was performed with the ADE4 software package [41] in R 1.9.0. Clusters were determined using hierarchical agglomerative clustering with average linkage in R1.9.0. ADE4 and R1.9.0 were downloaded from the Comprehensive R Archive Network (CRAN, http://cran.r-project.org). The Hellinger distance metric was used for PCA and cluster analysis.

Isolations. Isolates were obtained 10 days prior to the beginning of this study and on day 11 of this study. Serial dilutions of effluent and homogenized biofilms were plated on several different types of media: R2A, nutrient broth, Luria–Bertani (LB) medium, and filter sterilized reactor effluent supplemented with nitrate. Plates were incubated aerobically at 30°C. Morphologically distinct isolates were picked, restreaked to purity, and stored in 20% glycerol at −80°C.

Representative isolates of the distinct colony morphologies were identified by SSU rRNA sequence analysis. Cells were lysed by boiling in Tris–EDTA buffer for 5 min at 96°C. The SSU rRNA gene was amplified with the universal primers 8F and 1540R as previously described [14]. Prior to sequence determination, PCR reactions were treated with ExoSAP-IT™ (USB Corporation) according to the manufacturer's instructions. The primer 529r was used for sequence determination with a BigDye Terminator kit (Applied Biosystems) using a 3700 DNA analyzer (PerkinElmer) according to the manufacturer's instructions. SSU rRNA sequences were aligned with sequences from the RDP in ARB. The aligned sequences were inserted into the phylogenetic tree of RDP sequences in ARB using the parsimony method and nearest neighbors from the database were selected. A phylogenetic tree of isolate, clone, and database sequences was constructed as described above.

Isolates were assayed to determine their ability to denitrify. Batch denitrification assays were carried out in sealed anaerobic culture tubes with a helium headspace and the following media composition: 5 mM $NaNO_3$, 4.5 mM $C_3H_5NaO_3$ or C_2H_6O, 15 mM K_2HPO_4, 15 mM KH_2PO_4 and other nutrients in the same proportions as the FBR media.

Results

Functional Performance. Nitrogen removal was used as a metric of functional performance in this study and was computed as one minus the sum of the effluent concentrations of nitrate and nitrite divided by the influent nitrate concentration and was expressed as a percentage. Functional performance was monitored throughout the 370-day period of operation (Fig. 2).

During this period of operation, several disturbances and changes to operating conditions occurred that could arise in the field. To test the effect of a shutdown on functional performance and community structure in this system, a planned 17-day shutdown period was instituted from day 33 to 58. System shutdowns are sometimes

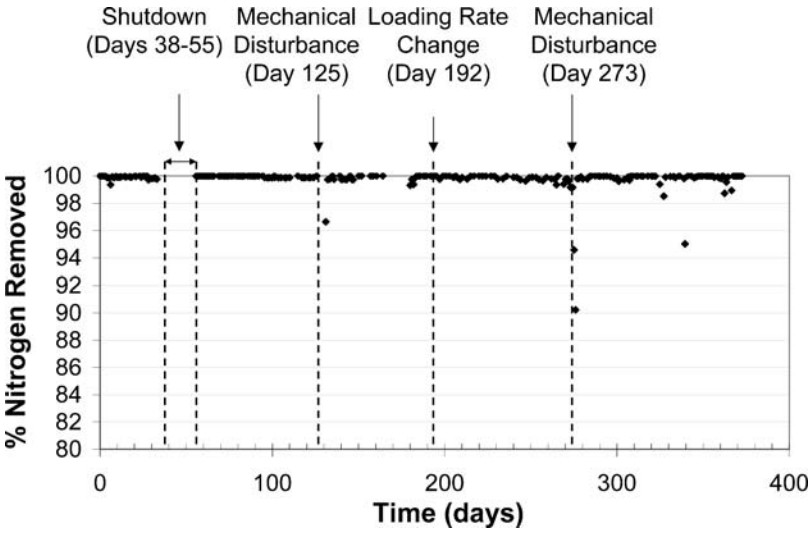

Figure 2. Functional performance of the denitrifying fluidized bed reactor. Nitrogen removal is one minus the sum of effluent concentrations of nitrate and nitrite divided by the influent nitrate concentration, expressed as a percentage.

required in practice when maintenance is being performed or during times when water does not need to be treated. On day 125, a pump failed, and air was pumped into the reactor, shearing biofilms from carrier particles. Many months later, on day 273, this disturbance was recreated by the purposeful mechanical shearing of biofilms from carrier particles. From days 180 to 192, the loading rate was increased roughly twofold through step increases in feed nitrate concentration.

During periods of constant operation, nitrogen removal was consistently greater than 99.3%, and this level of performance was not affected by the shutdown period or increase in loading rate. In contrast, lapses in performance did occur after the mechanical disturbances on days 125 and 273. Functional recovery from these instances was complete within 6 days. Nitrate removal decreased several times from day 300 to day 360, possibly the result of growth of fungal contaminant in the electron donor storage tank during this period.

The height of the fluidized bed is an indicator of biofilm growth because the buoyancy of carrier particles increases with increased biofilm thickness. After both of the mechanical disturbances, the height of the bed dropped as biofilms were stripped from carrier particles. The bed height recovered within 5 days of the disturbance on day 125 and 18 days after the disturbance on day 273.

Characterization of Community Structure

Clone Library. A clone library of the SSU rRNA gene was constructed with DNA extracted from the sample collected on day 25. The analysis revealed low diversity. Using a species definition of 97% sequence similarity, 10 operational taxonomic units (OTUs) were detected in the clone library and total richness was estimated to be 12 with the abundance-coverage estimator.

The majority of sequences were closely related to genera within the β-*Proteobacteria* including *Acidovorax* (96–100% sequence similarity to *Acidovorax* 3DHB1), *Zoogloea* (98–100% sequence similarity to *Zoogloea* DhA-35), and *Dechloromonas* (96% sequence similarity to *Dechloromonas* SUIL) (Fig. 3). A significant portion of sequences (17%) were closely related to the *Sporomusa* DR15 (96% sequence similarity) in the low G + C Gram-positive bacteria. In addition, a few clone sequences were related to *Dugenella zoogleoides* (92–96% sequence similarity) and *Xanthomonas campestris* (95% sequence similarity).

A large cluster of clone sequences related to *Acidovorax* species predominated the library, accounting for 44% of the sequences. One group of sequences in this cluster was closely related to *Acidovorax* 3DHB1 (98% sequence similarity), whereas a separate group of sequences was most closely related to *Acidovorax* G8B1 (96–100% sequence similarity). *Acidovorax* species have also been found in isolations and molecular inventories of many other denitrifying bioreactors and enrichment cultures [1, 10, 11, 26, 34, 38, 45, 46] and significant levels of *Acidovorax* have been measured in activated sludge by fluorescent *in situ* hybridization with *Acidovorax*-specific probes [1, 34].

Isolates. Partial SSU rRNA sequences were analyzed for 17 of the FBR isolates. The majority of isolates were related to *Acidovorax* 3DHB1 (99% similarity) and *Acidovorax* G8B1 (99% similarity). Despite the minor representation of clone sequences closely related to *D. zoogloeoides* and *X. campestris*, several isolates were closely related to these species (99% and 96% similarity, respectively). No representatives of the *Zoogloea* and *Dechloromonas*/*Dechlorosoma* clusters were isolated.

Functional assays of select isolates were performed to determine if they could reduce nitrate to nitrogen with lactate or ethanol as electron donors. Representative isolates were tested from clusters most closely related to *Acidovorax* (isolates G1, G2, S3, G17), *D. zoogloeoides* (isolate G7), and *Xanthomonas* (isolate S8). When lactate was provided as the electron donor, all isolates reduced nitrate to nitrogen, except for isolate G2, which reduced nitrate only to nitrite. None of the isolates were capable of nitrate reduction using ethanol as an electron donor.

Community Dynamics

Overall. The dynamics of the community over time are presented in Fig. 4 as a histogram of T-RF relative abundance for *Rsa*I T-RFLP profiles. Most T-RFs (the 117, 118, 475, 480, 489, 491, 582, 825, and 878 bp) were present throughout operation at consistent relative abundances during periods of constant operating conditions. These T-RFs, with the exception of the 475 and 825 bp T-RFs, were identified by correlation of fragment sizes to those predicted *in silico* from isolate and clone sequences (Fig. 3).

The 425-bp T-RF ranged in relative abundance from 21 to 58% and had the highest relative abundance in all profiles except on days 290, 307, and 339. This T-RF was associated with sequences from clones and isolates that clustered with *Acidovorax* species. *In silico* digestion of the clone sequences yielded predicted fragments of 427 or 428 bp. There was a 2- to 3-bp discrepancy between the 425-bp T-RF observed and the 427- and 428-bp *in silico* predictions from *Acidovorax*-like clones. This discrepancy is within the range that was observed in a detailed comparison of actual and predicted T-RF lengths [22].

T-RFLP of isolates G1 and G2 from within the *Acidovorax* cluster produced a dominant fragment at 425 bp, verifying assignment of this fragment to the *Acidovorax* cluster. Additional fragments appeared as minor

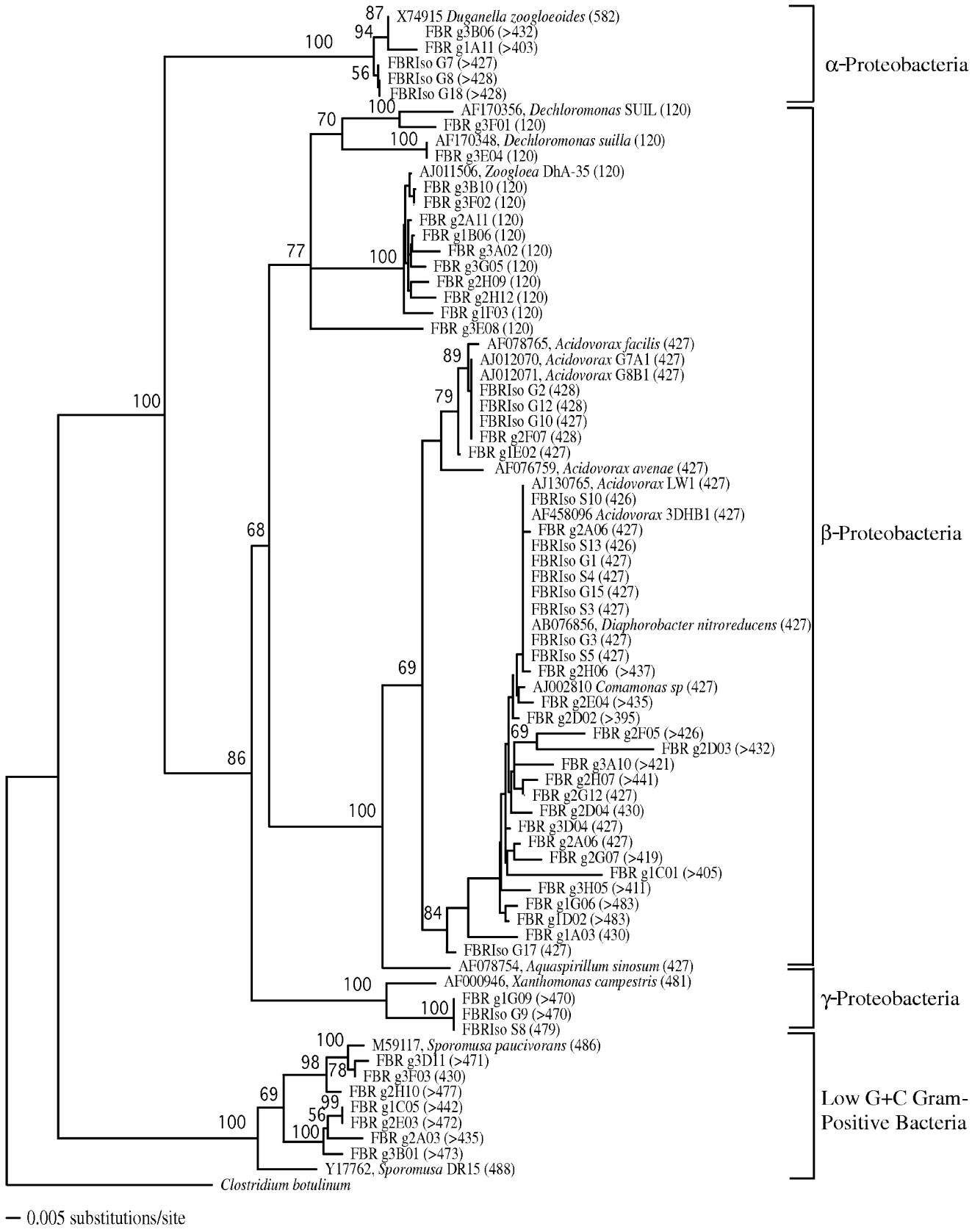
X74915 Duganella zoogloeoides (582)
FBR g3B06 (>432)
FBR g1A11 (>403)
FBRIso G7 (>427)
FBRIso G8 (>428)
FBRIso G18 (>428)
AF170356, Dechloromonas SUIL (120)
FBR g3F01 (120)
AF170348, Dechloromonas suilla (120)
FBR g3E04 (120)
AJ011506, Zoogloea DhA-35 (120)
FBR g3B10 (120)
FBR g3F02 (120)
FBR g2A11 (120)
FBR g1B06 (120)
FBR g3A02 (120)
FBR g3G05 (120)
FBR g2H09 (120)
FBR g2H12 (120)
FBR g1F03 (120)
FBR g3E08 (120)
AF078765, Acidovorax facilis (427)
AJ012070, Acidovorax G7A1 (427)
AJ012071, Acidovorax G8B1 (427)
FBRIso G2 (428)
FBRIso G12 (428)
FBRIso G10 (427)
FBR g2F07 (428)
FBR g1E02 (427)
AF076759, Acidovorax avenae (427)
AJ130765, Acidovorax LW1 (427)
FBRIso S10 (426)
AF458096 Acidovorax 3DHB1 (427)
FBR g2A06 (427)
FBRIso S13 (426)
FBRIso G1 (427)
FBRIso S4 (427)
FBRIso G15 (427)
FBRIso S3 (427)
AB076856, Diaphorobacter nitroreducens (427)
FBRIso G3 (427)
FBRIso S5 (427)
FBR g2H06 (>437)
AJ002810 Comamonas sp (427)
FBR g2E04 (>435)
FBR g2D02 (>395)
FBR g2F05 (>426)
FBR g2D03 (>432)
FBR g3A10 (>421)
FBR g2H07 (>441)
FBR g2G12 (427)
FBR g2D04 (430)
FBR g3D04 (427)
FBR g2A06 (427)
FBR g2G07 (>419)
FBR g1C01 (>405)
FBR g3H05 (>411)
FBR g1G06 (>483)
FBR g1D02 (>483)
FBR g1A03 (430)
FBRIso G17 (427)
AF078754, Aquaspirillum sinosum (427)
AF000946, Xanthomonas campestris (481)
FBR g1G09 (>470)
FBRIso G9 (>470)
FBRIso S8 (479)
M59117, Sporomusa paucivorans (486)
FBR g3D11 (>471)
FBR g3F03 (430)
FBR g2H10 (>477)
FBR g1C05 (>442)
FBR g2E03 (>472)
FBR g2A03 (>435)
FBR g3B01 (>473)
Y17762, Sporomusa DR15 (488)
Clostridium botulinum
α-Proteobacteria
β-Proteobacteria
γ-Proteobacteria
Low G+C Gram-Positive Bacteria
0.005 substitutions/site

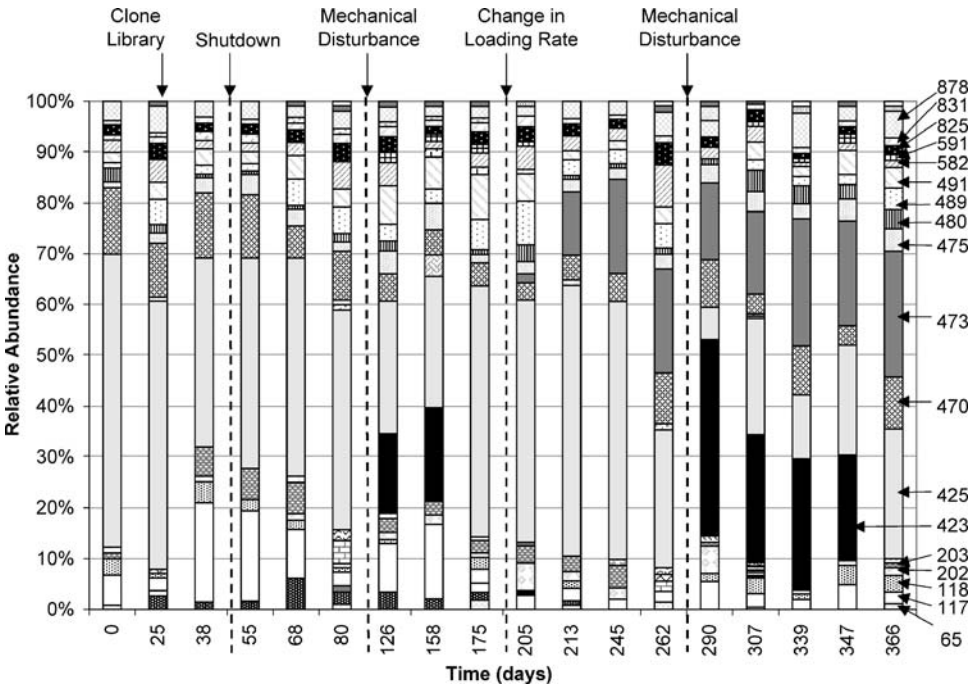

Figure 4. Histogram of T-RF relative abundances in *Rsa*I T-RFLP profiles of biofilm samples collected from the FBR over time. Relative abundance is the ratio of the peak height of a given T-RF in a given sample to the sum of all T-RFs in that sample, expressed as a percentage. *Arrows* indicate the size in base pairs of the restriction fragments for most T-RFs.

peaks in the T-RFLP analyses of these isolates. Minor peaks for fragment sizes 62, 470, and 878 bp were produced for isolate G1, and minor peaks for fragment sizes 198 and 470 bp were produced for isolate G2. These fragments are possibly due to multiple copies of the SSU rRNA gene on the genome [5] or the formation of pseudoterminal fragments [9]. Although the occurrence of several T-RFs for a single organism misrepresents the diversity of the community, the comparisons between samples made in this study are still meaningful, because the same biases apply to all samples.

Several other T-RFs were present throughout operation in lower relative abundances and were also correlated with sequences from the clone library. The restriction fragments for sequences related to *Dechloromonas* and *Zoogloea* are predicted to have a size of 120 bp. This likely correlates with the 117- or 118-bp OTUs that were detected throughout operation. OTUs for fragment sizes 480, 489, 491, and 582 bp could not be identified by correlation to clones in the library, because these lengths are greater than those of the clones (400–480 bp). However, predictions made from the longer, closely related sequences in the NCBI database and verified by digestions of selected samples with *Msp*I (data not shown) indicated that the 480-bp T-RF correlated with *Xanthomonas*, the 489- or 491-bp T-RFs with *Sporomusa*, and the 582-bp T-RF with *D. zoogloeoides*.

Effect of Loading Rate Increase and Shutdown. Despite the stability of community composition during periods of unvarying operating conditions, a significant change occurred after the roughly twofold increase in loading rate between days 180 and 192. Beginning with day 205, a previously undetected 473-bp T-RF appeared. By day 213, this T-RF had the second highest relative abundance and remained as one of the three T-RFs with the highest relative abundances for the duration of operation. This T-RF did not correlate with predicted T-RFs from any sequences in the clone library. The changes due to increased loading contrasted with the lack of any detectable change for the shutdown period from day 38 to day 55. Profiles from the month before the shutdown were similar to those observed in the month after the shutdown.

Effect of Disturbance. On days 125 and 273, biofilms were mechanically sheared from the carrier particles. Similar transient responses occurred after both disturbances, despite the difference in operating conditions

Figure 3. Phylogenetic analysis of partial SSU rRNA sequences. The tree was constructed with the neighbor-joining (*NJ*) method using sequences of 400 nucleotides. *Clostridium botulinum* is the outgroup species. The *scale bar* represents 0.005 nucleotide substitution per position. Bootstrap values below 50 are not shown. Numbered sequences are of the FBR clone library (*FBR*) and isolates from the FBR (*FBRIso*). Length of *in silico* restriction digests with *Rsa*I are given in parentheses. When no restriction site was found, the sequence is labeled (> clone sequence length).

and community structure observed prior to the disturbance. In both cases, a previously undetected 423-bp T-RF appeared concurrently with the decline in relative abundance of the dominant *Acidovorax*-like 425-bp T-RF. Subsequently, the 423-bp T-RF disappeared and the 425-bp T-RF returned to predisturbance levels. The two disturbances differed in the maximum relative abundance of the 423-bp T-RF. Following the first mechanical disturbance on day 125, the 423-bp T-RF appeared in samples from days 126 and 158 (1 and 24 days following the disturbance, respectively) and became the T-RF of second greatest relative abundance, with a maximum of 18.4%, in these samples. On day 175, 51 days postdisturbance, the 423-bp T-RF was no longer detected. After the second disturbance, the 423-bp T-RF remained in the profiles 74 days postdisturbance and did not disappear until day 366, 93 days after the disturbance. Additionally, the 423-bp T-RF surpassed the 425-bp T-RF as the dominant peak in profiles on days 290, 307, and 339 and obtained a maximum relative abundance of 38.5% on day 290.

Principal Component Analysis. The results of PCA and cluster analysis (Fig. 5) revealed the relative impact of the different disturbances on community structure. Reduction of the entire data set to the first two principal components accounted for 86% of the total variability. The PCA results are presented in two biplots (Fig. 5), one showing samples before, during, and after the first mechanical disturbance (A) and the other showing samples before, during, and after the second mechanical disturbance (B). Clusters determined by cluster analysis are circled on the PCA biplots. The cluster of samples from days 0 to 80 emphasized the minimal impact of the shutdown on community structure. Samples before each of the mechanical disturbances clustered together. Following both mechanical disturbances, samples deviated from the original cluster, indicating a change in structure. The community ultimately returned to the original cluster indicating the return to a predisturbance structure. The dominant, *Acidovorax*-like 425-bp T-RF had the highest loading on the first principal component 1 (Fig. 5C). The unidentified 423- and 473-bp T-RFs had the highest loadings on the second principal component (Fig. 5C), indicating that the appearances of previously undetected T-RFs were significant to overall community dynamics.

T-RFLP was performed on seven replicates from day 307. The replicates were composed of four PCR replicates of one DNA extraction and three PCR replicates of a separate extraction. The principal component coordinates for day 307 (± 95% confidence intervals) were (0.88 ± 0.02, −0.39 ± 0.02). These results suggest that the T-RFLP was sufficiently sensitive and reproducible to differentiate replicate samples from other closely related samples, as demonstrated by the error bars on day 307 in Fig. 5.

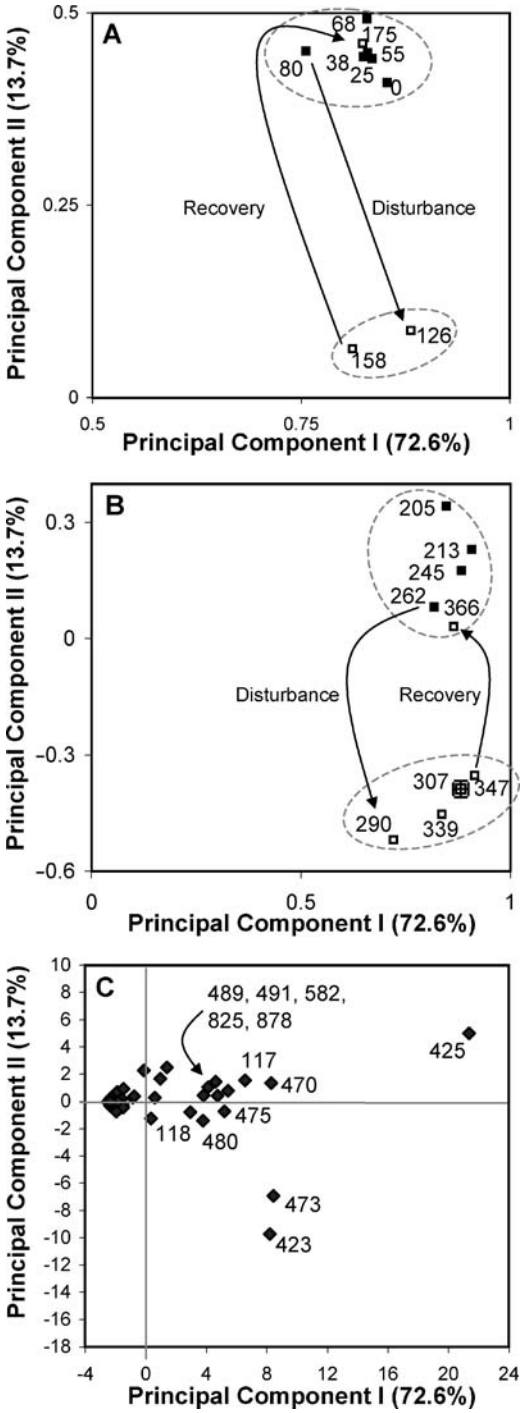

Figure 5. PCA analysis of the entire set of T-RFLP profiles based on relative T-RF abundance. (A) Score plot of samples before, during, and after the first disturbance. (B) Score plot of samples before, during, and after the second disturbance. *Closed squares*, samples before the disturbance. *Open squares*, samples after the disturbance. Of the total variability, 72.6% and 13.7% were accounted for by the first and second principal components, respectively. *Circles* indicate clusters determined by hierarchical agglomerative clustering with average linkages. (C) Loading plot: labels indicate T-RF length of T-RFs with high loadings.

Discussion

Functional Stability and Community Dynamics under Constant Operating Conditions. Under constant operating conditions, variability, the variance of community structure over time [32], and constancy, the property of staying essentially unchanged [16], are useful descriptors for characterizing the stability of community structure. In this investigation, the community was characterized by low variability and high constancy, because most T-RFs were present at fairly steady relative abundances in samples taken during periods of constant operating conditions. The constant microbial community was accompanied by functional stability. Microbial communities characterized by similarly high constancy and functional stability under constant operating conditions were also observed in a methanol-fed denitrifying FBR and a full-scale activated-sludge system treating pulp and paper mill wastewater [24, 35]. In contrast, highly variable community structure accompanied functional stability in a methanogenic dispersed growth reactor [12] and a methanogenic FBR [48]. In these systems, completely different populations dominated the community during different periods of operation and most populations were only transiently present.

The diversity was low in the highly constant systems, the FBR in this study, the methanol-fed FBR, and the activated sludge reactor. In this study the denitrifying FBR had an estimated richness of 12, whereas the methanol-fed denitrifying FBR and the activated sludge system had an estimated richness of 15 and between 12 and 16, respectively [24, 35]. In contrast, the variable bacterial community in the methanogenic FBR was extremely rich with 133 T-RFs observed in the clone library [15, 48]. Many ecologists now theorize that as diversity increases the variability of aggregate ecosystem properties (e.g., total biomass) decrease [7, 27, 28, 30, 42, 43], whereas the variability of individual populations may increase [27, 28, 30, 42]. This could explain the constancy of community structure observed in this work, because diversity was low, but it would not explain the stability of denitrification.

Functional stability could depend on how the function is packaged within and between species. It could remain high at low diversity if all of the enzymes needed for the function of interest can be packaged within one organism. This is the case for denitrification. In contrast, methanogenic communities degrade fermentable substrates by a variety of pathways, some linear and some branched, and the requisite enzymes are parsed among distinctive organisms. In such systems, shifts in pathways and community composition would be more probable.

Functional Stability and Community Dynamics in Response to Disturbances. In this investigation, the microbial community structure was not altered by a shutdown period of 17 days and the functional performance recovered quickly upon start-up after the shutdown. Similar results were observed after an 11-day shutdown in a full-scale activated-sludge system [35]. Community structure might be expected to change upon shutdown due to differences in decay rates among populations or differences in rates of biofilm detachment in fixed film systems, but these effects were not observed in the present study.

The community response to the mechanical disturbances observed in the present experiment had two interesting features: the community was disrupted and subsequently returned to its original state and the function recovered more quickly than the community structure. These behaviors were observed in response to both disturbances despite differences in community structure and operating conditions at the time of disturbance.

The transient presence of a new 423-bp T-RF following perturbation indicates a temporary change to conditions that favored that T-RF. After the first disturbance, the 423-bp T-RF appeared very quickly, just 1 day, after the shearing event, indicating that this T-RF was already present in the community. Perhaps this T-RF increased in relative abundance because it was more prevalent deeper within the biofilm in a region that remained after shearing. However, this T-RF remained at a substantial relative abundance for several weeks after the biofilms recovered, indicating that it was able to compete better after disturbances than during undisturbed operation.

In a study of methanogenic bioreactors, resilient function and community structure also correlated with the transient appearance of previously undetected populations, and authors hypothesized that "flexible" community structure promoted functional recovery [13, 17]. In that case, the temporary prevalence of the previously minor T-RF was attributed to its fast growth rate under briefly high substrate concentrations [13]. The similar community response observed in the current system despite application of an extremely different perturbation supports the hypothesis that flexible community structure and potentially the activity of populations present as minor members under nonperturbation conditions promotes system recovery.

In this study, both function and community structure were disrupted by the mechanical disturbances, but the time for recovery, as described by the ecological metric, resilience [17, 31], was on different scales. After both disturbances, nitrogen removal recovered within a few days, indicating a high functional resilience. This occurred despite the removal of a large amount of biomass in the disturbance. However, recovery of community structure was on the order of months, indicating low resilience of community structure. Slow recovery of community structure may reflect the amount

of time required for populations prevalent in biofilms during perturbation to be degraded. A similar observation was made for anaerobic digestors perturbed with glucose: Community structure resilience was at least seven times less than functional resilience [40]. Nitrate removal was efficient during the several weeks it took for the community structure to recover in the present study, indicating that this function did not depend on one particular community structure.

Acknowledgments

We thank Qi Ye for assistance in 16S rRNA sequencing of bacterial isolates. This research was supported by the Natural and Accelerated Bioremediation Research program, Biological and Environmental Research, U.S. Department of Energy under grant number DE-F603-00ER63046. Margaret Gentile was supported by a Stanford Graduate Fellowship sponsored by James Clark and a fellowship from the U.S. Environmental Protection Agency Science to Achieve Results program.

References

1. Amann, R, Ludwig, W, Schulze, R, Spring, S, Moore, E, Schleifer, KH (1996) rRNA-targeted oligonucleotide probes for the identification of genuine and former pseudomonads. Syst Appl Microbiol 19: 501–509
2. Briones, A, Raskin, L (2003) Diversity and dynamics of microbial communities in engineered environments and their implications for process stability. Curr Opin Biotechnol 14: 270–276
3. Cole, JR, Chai, B, Marsh, TL, Farris, RJ, Wang, Q, Kulam, SA, Chandra, S, Mcgarrell, DM, Schmidt, TM, Garrity, GM, Tiedje, JM (2003) The ribosomal database project (RDP-II): previewing a new autoaligner that allows regular updates and the new prokaryotic taxonomy. Nucleic Acids Res 31: 442–443
4. Colwell, RK (2004) EstimateS: Statistical Estimation of Species Richness and Shared Species from Samples. Version 7 [Online.]. User's guide and application available at: http://Purl.Oclc.Org/Estimates
5. Crosby, LD, Criddle, CS (2003) Understanding bias in microbial community analysis techniques due to rrn operon copy number heterogeneity. Biotechniques 34: 790–802
6. Curtis, T, Head, I, Graham, D (2003) Theoretical ecology for engineering biology. Environ Sci Technol 37: 64A–70A
7. Doak, DF, Bigger, D, Harding, EK, Marvier, MA, O'Malley, RE, Thomson, D (1998) The statistical inevitability of stability–diversity relationships in community ecology. Am Natural 151: 264–276
8. Dunbar, J, Ticknor, L, Kuske, C (2000) Assessment of microbial diversity in four southwestern United States soils by 16S rRNA gene terminal restriction fragment analysis. Appl Environ Microbiol 66: 2943–2950
9. Egert, M, Friedrich, M (2003) Formation of pseudo-terminal restriction fragments, a PCR-related bias affecting terminal restriction fragment length polymorphism analysis of microbial community structure. Appl Environ Microbiol 69: 2555–2562
10. Etchebehere, C, Errazquin, I, Barrandeguy, E, Dabert, P, Moletta, L, Muxi, L (2001) Evaluation of the denitrifying microbiota of anoxic reactors. FEMS Microbiol Ecol 35: 259–265
11. Etchebehere, C, Errazquin, M, Dabert, P, Muxi, L (2002) Community analysis of a denitrifying reactor treating landfill leachate. FEMS Microbiol Ecol 40: 97–106
12. Fernandez, A, Huang, SY, Seston, S, Xing, J, Hickey, R, Criddle, C, Tiedje, J (1999) How stable is stable? Function *versus* community composition. Appl Environ Microbiol 65: 3697–3704
13. Fernandez, AS, Hashsham, SA, Dollhopf, SL, Raskin, L, Glagoleva, O, Dazzo, O, Hickey, RF, Criddle, CS, Tiedje, JM (2000) Flexible community structure correlates with stable community function in methanogenic bioreactor communities perturbed by glucose. Appl Environ Microbiol 66: 4058–4067
14. Fields, MW, Yan, T, Rhee, S-K, Carroll, SL, Jardine, PM, Watson, DB, Criddle, DB, Zhou, J (2005) Impacts on microbial communities and cultivable isolates from groundwater contaminated with high levels of nitric acid–uranium waste. FEMS Microbiol Ecol 53: 417–428
15. Godon, JJ, Zumstein, E, Dabert, P, Habouzit, F, Moletta, R (1997) Molecular microbial diversity of an anaerobic digestor as determined by small-subunit rDNA sequence analysis. Appl Environ Microbiol 63: 2802–2813
16. Grimm, V, Schmidt, E, Wissel, C (1992) On the application of stability concepts in ecology. Ecol Model 63: 143–161
17. Hashsham, S, Fernandez, A, Dollhopf, S, Dazzo, F, Hickey, R, Tiedje, J, Criddle, J (2000) Parallel processing of substrate correlates with greater functional stability in methanogenic bioreactor communities perturbed by glucose. Appl Environ Microbiol 66: 4050–4057
18. Hiscock, K, Lloyd, J, Lerner, D (1991) Review of natural and artificial denitrification of groundwater. Water Res 25: 1099–1111
19. http://www.esd.ornl.gov/Nabirfrc/. Cited November 19, 2004
20. Hurt, RA, Qiu, XY, Wu, LY, Roh, Y, Palumbo, AV, Tiedje, JM, Zhou, JH (2001) Simultaneous recovery of RNA and DNA from soils and sediments. Appl Environ Microbiol 67: 4495–4503
21. Janda, V, Rudovsky, J, Wanner, J, Marha, K (1988) *In situ* denitrification of drinking-water. Water Sci Technol 20: 215–219
22. Kaplan, C, Kitts, C (2003) Variation between observed and true terminal restriction fragment length is dependent on true TRF length and purine content. J Microbiol Methods 54: 121–125
23. Kaplan, CW, Astaire, JC, Sanders, ME, Reddy, BS, Kitts, CL (2001) 16S ribosomal DNA terminal restriction fragment pattern analysis of bacterial communities in feces of rats fed lactobacillus acidophilus NCFM. Appl Environ Microbiol 67: 1935–1939
24. Labbe, N, Juteau, P, Parent, S, Villemur, R (2003) Bacterial diversity in a marine methanol-fed denitrification reactor at the Montreal Biodome, Canada. Microbial Ecol 46: 12–21
25. Lane, D (1991) 16S/23s rRNA sequencing. In: Stackebrant E, Goodfellow M (Eds.) Nucleic Acid Techniques in Bacterial Systematics. Wiley, New York, pp 115–175
26. Lee, H, Lee, S, Lee, J, Park, J, Choi, E, Park, Y (2002) Molecular characterization of microbial community in nitrate-removing activated sludge. FEMS Microbiol Ecol 41: 85–94
27. Lehman, CL, Tilman, D (2000) Biodiversity, stability, and productivity in competitive communities. Am Nat 156: 534–552
28. Loreau, M, Naeem, S, Inchausti, P, Bengtsson, J, Grime, J, Hector, A, Hooper, A, Huston, M, Raffaelli, D, Schmid, B, Tilman, D, Wardle, D (2001) Ecology—biodiversity and ecosystem functioning: current knowledge and future challenges. Science 294: 804–808
29. Ludwig, W, Strunk, O, Westram, R, Richter, L, Meier, H, Kumar, Y, Buchner, A, Lai, T, Steppi, S, J obb, G, Forster, W, Brettske, W, Gerber, S, Ginhart, AW, Gross, O, Grumann, S, Hermann, S, Jost, R, Konig, A, Liss, T, Lussmann, R, May, M, Nonhoff, B, Reichel, B, Strehlow, R, Stamatakis, A, Stuckmann, N, Vilbig, A, Lenke, M, Ludwig, T, Bode, A, Schleifer, KH (2004) ARB: a software environment for sequence data. Nucleic Acids Res 32: 1363–1371

30. Mcnaughton, SJ (1977) Diversity and stability of ecological communities a comment on the role of empiricism in ecology. Am Nat 111: 515–525
31. Neubert, M, Caswell, H (1997) Alternatives to resilience for measuring the responses of ecological systems to perturbations. Ecology 78: 653–665
32. Pimm, S (1984) The complexity and stability of ecosystems. Nature 307: 321–326
33. Qiu, XY, Wu, LY, Huang, HS, McDonel, PE, Palumbo, AV, Tiedje, JM, Zhou, JM (2001) Evaluation of PCR-generated chimeras: mutations, and heteroduplexes with 16S rRNA gene-based cloning. Appl Environ Microbiol 67: 880–887
34. Schulze, R, Spring, S, Amann, R, Huber, I, Ludwig, W, Schleifer, KH, Kampfer, KH (1999) Genotypic diversity of acidovorax strains isolated from activated sludge and description of *Acidovorax defluvii* sp nov. Syst Appl Microbiol 22: 205–214
35. Smith, N, Yu, Z, Mohn, W (2003) Stability of the bacterial community in a pulp mill effluent treatment system during normal operation and a system shutdown. Water Res 37: 4873–4884
36. Smith, R, Miller, D, Brooks, M, Widdowson, M, Killingstad, M (2001) *In situ* stimulation of groundwater denitrification with formate to remediate nitrate contamination. Environ Sci Technol 35: 196–203
37. Son, K, Hall, E (2003) Use of a similarity index based on microbial fatty acid (MFA) analysis to monitor biological wastewater treatment systems. Environ Technol 24: 1147–1156
38. Song, BK, Palleroni, NJ, Haggblom, MM (2000) Isolation and characterization of diverse halobenzoate-degrading denitrifying bacteria from soils and sediments. Appl Environ Microbiol 66: 3446–3453
39. Stamper, D, Walch, M, Jacobs, R (2003) Bacterial population changes in a membrane bioreactor for graywater treatment monitored by denaturing gradient gel electrophoretic analysis of 16S rRNA gene fragments. Appl Environ Microbiol 69: 852–860
40. Sundh, I, Carlsson, H, Nordberg, A, Hansson, M, Mathisen, B (2003) Effects of glucose overloading on microbial community structure and biogas production in a laboratory-scale anaerobic digester. Bioresour Technol 89: 237–243
41. Thioulouse, J, Chessel, D, Doledec, S, Olivier, J-M (1997) Ade-4: a multivariate analysis and graphical display software. Stat Comput 7: 75–83
42. Tilman, D (1996) Biodiversity: population *versus* ecosystem stability. Ecology 77: 350–363
43. Tilman, D (1999) The ecological consequences of changes in biodiversity: a search for general principles. Ecology 80: 1455–1474
44. Von Canstein, H, Li, Y, Felske, A, Wagner-Dobler, I (2001) Long-term stability of mercury-reducing microbial biofilm communities analyzed by 16S-23s rDNA interspacer region polymorphism. Microbial Ecol 42: 624–634
45. Wang, CC, Lee, CM (2001) Denitrification with acrylonitrile as a substrate using pure bacteria cultures isolated from acrylonitrile–butadiene–styrene wastewater. Environ Int 26: 237–241
46. Yoshie, S, Noda, N, Miyano, T, Tsuneda, S, Hirata, A, Inamori, Y (2001) Microbial community analysis in the denitrification process of saline-wastewater by denaturing gradient gel electrophoresis of PCR-amplified 16S rDNA and the cultivation method. J Biosci Bioeng 92: 346–353
47. Zhou, JZ, Bruns, MA, Tiedje, JM (1996) DNA recovery from soils of diverse composition. Appl Environ Microbiol 62: 316–322
48. Zumstein, E, Moletta, R, Godon, JJ (2000) Examination of two years of community dynamics in an anaerobic bioreactor using fluorescence polymerase chain reaction (PCR) single-strand conformation polymorphism analysis. Environ Microbiol 2: 69–78